Available online at www.sciencedirect.com
ScienceDirect
Trans. Nonferrous Met. Soc. China 27(2017) 25−35
Transactions of Nonferrous Metals Society of China
www.tnmsc.cn

Fabrication and performance evaluation of dissimilar magnesium−aluminium alloy multi-seam friction stir clad joints

A. K. LAKSHMINARAYANAN; V. E. ANNAMALAI

Department of Mechanical Engineering, SSN College of Engineering, Kalavakkam, Chennai 603110, Tamil Nadu, India

Received 29 December 2015; accepted 7 May 2016

Abstract: This investigation is aimed to establish empirical relationships between continuous multi-seam friction stir cladding process parameters (i.e., rotational speed, welding speed and shoulder overlap ratio) and the quality characteristics (bond tensile strength, shear strength and corrosion) of dissimilar magnesium−aluminium alloy clad joints. The influence of considered process parameters on the clad properties was reported. Furthermore, multi-criterion optimization procedure was used to obtain ideal processing conditions, which can yield higher interface strength and lower corrosion rate of fabricated composite plate. Results indicate that, the aluminium-rich thin continuous layer, Mg-rich irregular shaped regions consists of Al_3Mg_2 and $Al_{12}Mg_{17}$ intermetallic compounds and nature of mechanical interlocking has great influence on the joint interface strength. On the other hand, the corrosion resistance of the clad joints is greatly affected by the amount of magnesium mixed with top aluminium sheet during friction stirring. Also, bend testing shows that, the cladded joints exhibit excellent ductility.

Key words: friction stir cladding; dissimilar joint; overlap ratio; optimization

1 Introduction

Magnesium and its alloys find extensive use in automotive and aerospace structures due to its attractive characteristics such as low density, high specific strength, decent heat dissipation and better damping capacity [1]. However, it suffers from poor corrosion resistance due to its airy natural outer surface layer [2]. Hence, the top layer needs to be modified to improve its surface properties. Among the various techniques attempted by the researchers to enhance the corrosion resistance, deposition of thin aluminium layer on the magnesium plates is considered as a successful approach. Magnesium (Mg) covered with thin aluminium (Al) layer is an attractive combination for automotive applications (e.g. multi-material light weight vehicles). Methods available for fabricating this combination are various types of coatings such as chemical conversion, anodic oxidation, organic coating, electrochemical coating, thermal spraying, laser cladding and solid state processes such as diffusion bonding, accumulative roll bonding, hot pressing, explosive cladding and equal channel angular processing [3−12]. Cracks and porosity are unavoidable in coatings and they deteriorate both the mechanical and corrosion resistances. Moreover, chemical conversion coatings are toxic and not an eco-friendly technique. Diffusion bonding and hot pressing techniques need longer time to obtain a metallurgical bond and also these joints exhibited very low strength due to the high temperature exposure. Similarly, accumulative roll bonded joints are prone to grain coarsening and cracking at the intermetallic matrix interface and subsequently offered inferior joint properties. Equal channel angular extruded dissimilar joints need additional heat treatment to minimize detrimental phases at the joint interface. Explosive cladding is very effective in controlling the formation of intermetallic compounds; however, its application for dissimilar Al−Mg cladding is limited due to the safety issues, bulk material joining (i.e., need sufficiently thick top sheet), working hardening due to sudden impact forces, inhomogeneous microstructure and higher tensile residual stresses.

An alternate process of joining aluminium to magnesium alloy is friction stir welding, which is gaining importance nowadays; however, the current literature mostly concerns on the butt and single seam lap

Corresponding author: A. K. LAKSHMINARAYANAN; Tel: +91-44-27469700-236; Fax: +91-44-27469772; E-mail: LakshminarayananAK@ssn.edu.in
DOI: 10.1016/S1003-6326(17)60004-9

joint configurations [13,14]. Recently, few attempts were made to develop an alternative cladding technique based on multi-seam friction stir lap welding, which showed enhanced joint properties and minimized physical and metallurgical deficiencies compared with conventional cladding processes. LIU et al [15] conducted a preliminary study on the microstructure and corrosion resistance of friction stir processed AZ80/Al composite plate and observed that a dense composite Al layer with superfine and uniform grains was formed, and a few intermetallic compounds existed in the area of Mg/Al interface.

GANESA BALAMURUGAN and MAHADEVAN [16] studied the effect of parameters, namely, rotational speed and welding speed on the uniaxial tensile strength and corrosion resistance of friction stir cladded AA5083−AZ31B magnesium composite plate and reported that the clads fabricated with higher rotational and welding speeds showed inferior uniaxial tensile strength and lower corrosion resistance. However, to obtain the interface properties, it is essential to evaluate the bonding strength (BS) and shear strength (SS) in a systematic manner. Moreover, in friction stir cladding, the other most influencing process parameter, which decides that the bonding strength is overlap area, which was not considered in their study. Hence, in this investigation, a three-factor (i.e., rotational speed, welding speed and shoulder overlap ratio), five-level central composite rotatable design matrix was used to fabricate AZ31B magnesium alloy−AA5052 aluminium composite plate using multi-seam friction stir welding. Empirical relationships between controlling factors and quality characteristics were developed and the influences of process factors on the shear strength, bonding strength and corrosion resistance were studied. Further, the best possible combination of process parameters which can yield maximum shear strength, bonding strength and lower corrosion rate (CR) was identified using multi-response optimization procedure. Under optimum conditions, bend test was performed to confirm the integrity and ductility of cladded composite plate.

2 Experimental

2.1 Primary process parameters and their range

Though many primary and secondary factors affect the quality characteristics of friction stir lap welded aluminium−magnesium dissimilar joints, it is clearly evidenced from Ref. [17] that the process factors such as rotational speed and welding speed affect the weld nugget consolidation, intermetallic formation, intercalated band structure, grain size, mechanical and metallurgical properties. However, for multi-seam friction stir lap welding to clad aluminium sheet on magnesium plates, overlap area between two seams is an important factor, which decides the joint integrity. Hence, tool rotational speed, welding speed and overlap area are considered in this investigation.

2.2 Feasible working limits of process parameters

In this study, commercially available 6 mm-thick AZ31B magnesium alloy and 1.5 mm-thick AA5052 aluminium alloy were used. Before welding, the surface of the plates was ground with fine emery papers to remove the oxide film and cleaned with ethanol. Both aluminium and magnesium alloys were cut and machined to dimensions of 140 mm ×100 mm. The Al alloy sheet was overlaid on the lower Mg alloy plate, which was firmly clamped to an anvil. Before fixing the range of process factors selected, multi-seam friction stir passes were made using a tool without pin to get closer contact of aluminium with magnesium to facilitate solid state bonding (Fig. 1(a)). For further experiments, H13 alloy tools with a shoulder diameter of 12 mm, pin diameter of 3 mm and a length of 2.6 mm were used. To establish the range of rotational speed and welding speed, each of them was varied from the minimum to maximum with no overlap ratio used. The feasible working limits were fixed based on the visual inspection, considering sheet separation, non-uniform weld bead profile, excessive flash formation, surface defects, and sub-surface voids. The outcome of the above analysis is summarized in Table 1.

The upper and lower limits of process parameters were 1.682 and −1.682, respectively, and the coded values were calculated by

$$X_i = \frac{1.682[2X - (X_{\max} + X_{\min})]}{(X_{\max} + X_{\min})} \quad (1)$$

where X_i is the coded value of a variable X which varies from $X_{\min}$ to $X_{\max}$. The working limits of process parameters with its range are presented in Table 2. It is important to note that, the overlap ratio was varied between the entire possible limits of 0 to 100%.

2.3 Multi-seam friction stir cladding experiments as per design matrix

A three-factor, five-level, central composite rotatable design matrix (Table 3) was used to carry out the multi-seam friction stir cladding experiments. As mentioned earlier, the shoulder overlap ratio was varied and the cladded Al−Mg composite plates at different overlap ratios are presented in Figs. 1(b)−(f). All the claddings were done using continuous multi-seam welding method in which, each pass was uninterruptedly completed with no cooling time allowed between passes.

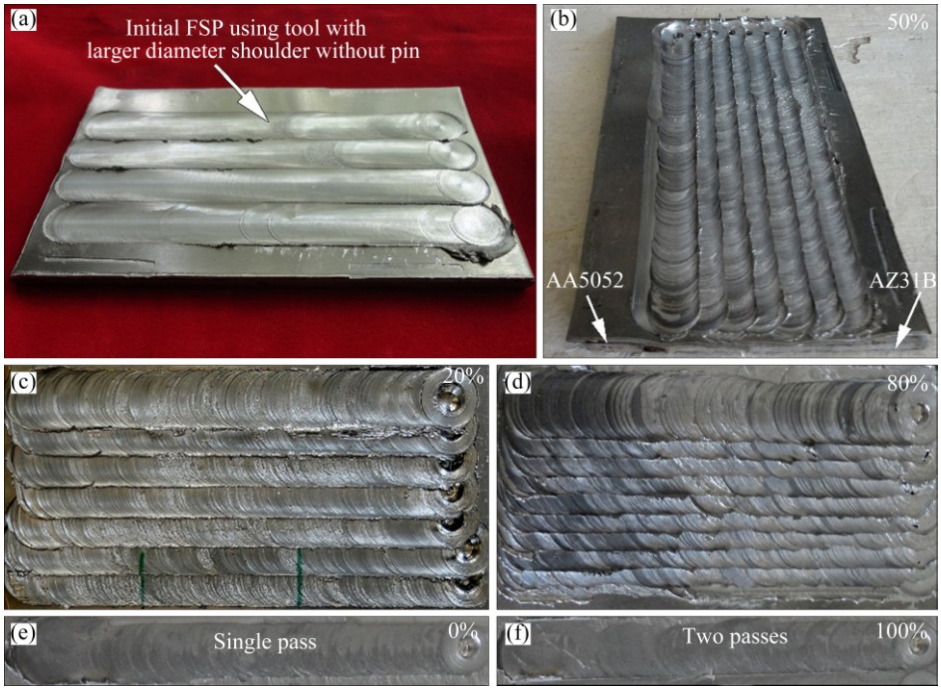

Fig. 1 Fabricated joints showing different overlap ratios (other factors at mid-level)

Table 1 Establishing feasible limits of process parameters

Parameter	Selection	Macrostructure	Inference
Rotational speed	<400 r/min	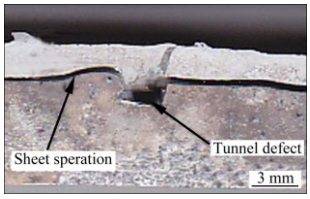	Tunnel at the root, sheet separation – insufficient heat generation and inadequate material flow to obtain metallurgical bonding at the interface
	>1000 r/min	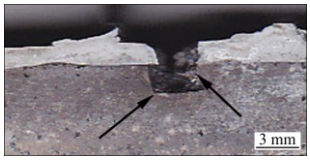	Excessive discharge of plasticized aluminium top sheet in plunge region due to turbulent flow at higher rotational speed
Welding speed	< 30 mm/min		A tunnel defect at the Mg/Al interface in pin influenced region. High heat generation and higher viscoplastic material flow due to lower welding speed
	> 70 mm/min		Groove defect—Inadequate frictional heat generation and lower exposure time to obtain a metallurgical bond between Al/Mg due to higher welding speed

Table 2 Range and its level of influencing process parameters

Factor	Symbol	Level				
		−1.682	−1	0	1	1.682
Rotational speed/(r·min^{-1})	v_r	600	681	800	919	1000
Welding speed/(mm·min^{-1})	v_w	30	38	50	62	70
Shoulder overlap ratio/%	R_o	0	20	50	80	100

2.4 Properties of fabricated composite plate

Specimens for evaluating bond tensile strength (σ_b), shear strength (σ_c), bend strength (σ), metallographic analysis were prepared from cladded composite plates using wire cut electrical discharge machine. Metallographic samples were polished with different abrasive grade sheets and etched with a solution containing 5 mL acetic acid, 6 g picric acid, 10 mL water and 100 mL ethanol to capture the cross sectional

Table 3 Experimental design matrix with evaluated data

No	Coded value			Actual Value			σ_b/MPa	σ_c/MPa	r_c/(10^{-3} mm·a^{-1})
	v_r	v_w	R_o	v_r	v_w	R_o			
1	−1	−1	−1	681	38	20	63	23	4.21
2	+1	−1	−1	919	38	20	65	27	4.78
3	−1	+1	−1	681	62	20	76	36	1.40
4	+1	+1	−1	919	62	20	74	33	4.74
5	−1	−1	+1	681	38	80	83	42	5.24
6	+1	−1	+1	919	38	80	72	36	3.77
7	−1	+1	+1	681	62	80	88	45	2.99
8	+1	+1	+1	919	62	80	73	32	4.57
9	−1.682	0	0	600	50	50	77	34	3.03
10	1.682	0	0	1000	50	50	65	27	4.83
11	0	−1.682	0	800	30	50	73	36	4.89
12	0	1.682	0	800	70	50	85	43	2.97
13	0	0	−1.682	800	50	0	66	27	3.57
14	0	0	1.682	800	50	100	83	44	4.28
15	0	0	0	800	50	50	82	40	3.68
16	0	0	0	800	50	50	83	42	3.81
17	0	0	0	800	50	50	82	42	3.54
18	0	0	0	800	50	50	83	42	3.55
19	0	0	0	800	50	50	82	42	3.61
20	0	0	0	800	50	50	82	40	3.58

macrostructure and microstructure. The ram tensile test (Fig. 2(a)) and interface shear test (Fig. 2(b)) were carried out at room temperature at a crosshead speed of 1 mm/min using a universal tensile testing machine to record the bonding and shear strength of the fabricated composite plate.

Three samples were tested under each condition as dictated by design matrix and the average values were recorded (Table 3). A temperature controllable salt spray chamber in conjunction with an air compressor was used for corrosion testing. The ripples formed on the aluminium top surface due to friction stir cladding was mechanically ground and polished as per standard metallographic procedure to a surface finish of 10 μm. The samples of 20 mm × 15 mm × 7.3 mm were suspended with nylon string in the chamber in such a way that, the cladded aluminium top surface was exposed to salt fog mist and other magnesium sides were covered with acid resisting cover tapes to avoid errors in the mass loss measurements. A 3.5% NaCl aqueous solution with constant pH value of 7.0 was prepared and the test was carried out for a spraying time of 45 min at the room temperature. Corrosion rate (r_c) was measured using a mass loss method as prescribed by ASTM B117 standard. The cross sectional microstructure of the

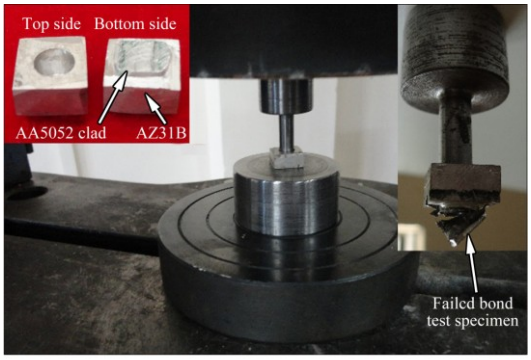

(a)

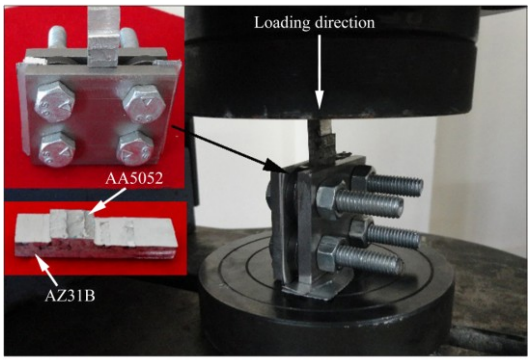

(b)

Fig. 2 Sample and fixture used for mechanic testing: (a) Ram tensile test; (b) Shear test

as-cladded and bent specimens was analyzed using optical and scanning electron microscopy.

3 Establishing parametric-response relationships

The quality characteristics such as bond tensile strength (σ_b), shear strength (σ_c), and corrosion rate (r_c) of multi-seam friction stir cladded magnesium–aluminium composite largely depend on the process parameters, namely rotational speed (v_r), welding speed (v_w) and tool shoulder overlap ratio (R_o) respectively and the response functions are represented as given in Eq. (2).

$$\sigma_b,\ \sigma_c,\ r_c=f(v_r,\ v_w,\ R_o) \quad (2)$$

The second order response surface models were developed using Design Expert V.8.1 and are given in Eqs. (3)−(6). The procedure for establishing such relationships can be dealt elsewhere [18].

An empirical response surface model for predicting bond tensile strength is presented in Eq. (3).

$$\sigma_b=\{82.33-2.79v_r+3.60v_w-2.38R_o-0.87v_rv_w-6.37v_rR_o+0.63v_wR_o-4.50v_r^2-2.21v_w^2-2.56R_o^2\} \quad (3)$$

An empirical response surface model for predicting shear strength is presented in Eq. (4).

$$\sigma_c=\{42.51-2.03v_r+2.45v_w-1.47R_o-1.50v_rv_w-5.25v_rR_o-1.25v_wR-3.94v_r^2-1.99v_w^2-1.99R_o^2\} \quad (4)$$

An empirical response surface model for predicting the corrosion rate is presented in Eq. (5).

$$r_c=\{3.63+0.52v_r-0.55v_w+0.19R_o+0.73v_rv_w-0.47v_rR_o+0.18v_wR_o+0.11v_r^2+0.11v_w^2+0.11R_o^2\}\times10^{-3} \quad (5)$$

3.1 Verifying adequacy of developed models using ANOVA

The adequacy of the developed empirical relationships was tested using the analysis of variance (ANOVA) and the second order response surface model fitted in the form of ANOVA is presented in Table 4.

The model F values of 718.29, 86.08, and 227.52 imply that, the developed models for bond tensile strength, shear strength and corrosion rate respectively are significant. Values of prob>F less than 0.05 indicate that, the model terms of respective responses are significant. The results clearly indicate that, all the considered factors are significant. Lack of fit for all models is not significant as non-significant lack of fit is good. Adequate precision is the measure of signal to noise ratio and the value greater than 4 is desirable. The values of 92, 23 and 64 indicate the adequate signal for bonding tensile strength, shear strength, and corrosion rate respectively. The determination coefficient (R^2) is in the range of 0.98−0.99, which indicates the goodness of fit for the developed models of all three responses.

3.2 Model validating experiments

Friction stir cladding experiments were carried out

Table 4 Analysis of variance for four responses

Term	Bond tensile strength		Shear strength		Corrosion rate	
	F-value	p-value, Prob>F	F value	p-value, Prob>F	F value	p-value, Prob>F
Model	718.2921	< 0.0001	86.08479	< 0.0001	227.5199	< 0.0001
v_r	632.5736	< 0.0001	61.57545	< 0.0001	496.051	< 0.0001
v_w	1052.062	< 0.0001	89.34722	< 0.0001	566.1992	< 0.0001
R_o	458.1243	< 0.0001	32.2232	0.0002	69.30194	< 0.0001
v_rv_w	36.38266	0.0001	19.62453	0.0013	577.5591	< 0.0001
v_rR_o	1931.251	< 0.0001	240.4005	< 0.0001	246.2168	< 0.0001
v_rR_o	18.56258	0.0015	13.62814	0.0042	33.42001	0.0002
v_r^2	1736.036	< 0.0001	243.3981	< 0.0001	23.79723	0.0006
v_w^2	416.2937	< 0.0001	62.30553	< 0.0001	23.79723	0.0006
R_o^2	560.4786	< 0.0001	62.30553	< 0.0001	23.03867	0.0007
Lack of fit	0.262621	0.9157	0.222959	0.9374	0.402156	0.8299
R^2	0.9985		0.9873		0.9951	
Pred R-squared	0.9956		0.9663		0.9834	
Adeq precision	92.39		25.94		64.30	
Significant	Yes		Yes		Yes	
Lack of fit	Insignificant		Insignificant		Insignificant	

for a randomly selected three sets of parameters in the range of process parameters to validate the response surface equations (Eqs. (3)−(5)). The parameters were selected by such a way that, these are not available in the design matrix. The outcomes of validation experiments presented in Table 5 were quite satisfactory with a prediction error less than 10%.

4 Results and discussion

In cladded composite plates, the interfacial bonding between the two materials decides the overall mechanical integrity. Similarly corrosion resistance of aluminium cladded magnesium alloy depends on the percentage of substrate dilution on the top layer. In friction stir cladding, both interfacial strength and corrosion resistance depend on the process parameters, namely rotational speed, welding speed and shoulder overlap ratio.

The interfacial strength was evaluated using ram tensile strength and compressive shear test and the effects of the individual process parameters are displayed in Fig. 3.

These graphs were obtained by plotting each response with respect to the individual parameter by keeping other parameters at their mid value. It is clear that, the bond and shear strength increased with the increase of rotational speed, welding speed and overlap ratio and reaching the maximum and then decreased with the increase of each individual process parameter. This can be correlated with the interface microstructure, which is affected by difference in the plastic deformation assisted frictional heat caused by the parametric changes. At lower rotational speed of 600 r/min, the generated frictional heat and the peak temperature attained were insufficient to plasticize the top aluminium sheet, which caused improper mixing at the magnesium−aluminium interface (Fig. 4(a)). This subsequently ended into a nonuniform aluminium flow into the magnesium bottom plate and led to weaker bonding with defect at the interface. On the other hand, higher rotational speed of 1000 r/min with excessive stirring led to detachment of aluminium fragments from the top aluminum sheet, which were then indecorously dispersed in magnesium alloy side. Also, the turbulence caused by higher rotational speed hindered the movement of plasticized magnesium alloy into sharp edges of aluminium fragments, which led to the formation of voids and micro-cracks (Fig. 4(b)). This is the reason for lower bond strength at higher rotational speed. Similarly, too low or too high welding speed affected the metallurgical bonding at the aluminium and magnesium interface.

Table 5 Model justification experiments

No.	v_r/ (r·min^{-1})	v_w/ (mm·min^{-1})	R_o/ mm	Bonding strength/MPa			Shear strength/MPa			Corrosion rate/ (10^{-3} mm·a^{-1})		
				Actual/%	Predicted	Error/%	Actual/%	Predicted	Error/%	Actual/%	Predicted	Error/%
1	800 (0.00)	65 (1.25)	20 (−1)	79.55	82.41	−3.59	40.00	43.51	−8.78	2.68	2.81	−4.85
2	740 (−0.50)	56 (−0.50)	28 (1.50)	70.11	75.01	−6.98	36.00	38.64	−7.33	4.82	4.63	3.94
3	889 (0.75)	44 (0.50)	43 (−0.25)	82.28	80.18	−2.55	41.55	40.32	2.96	4.50	4.13	8.22

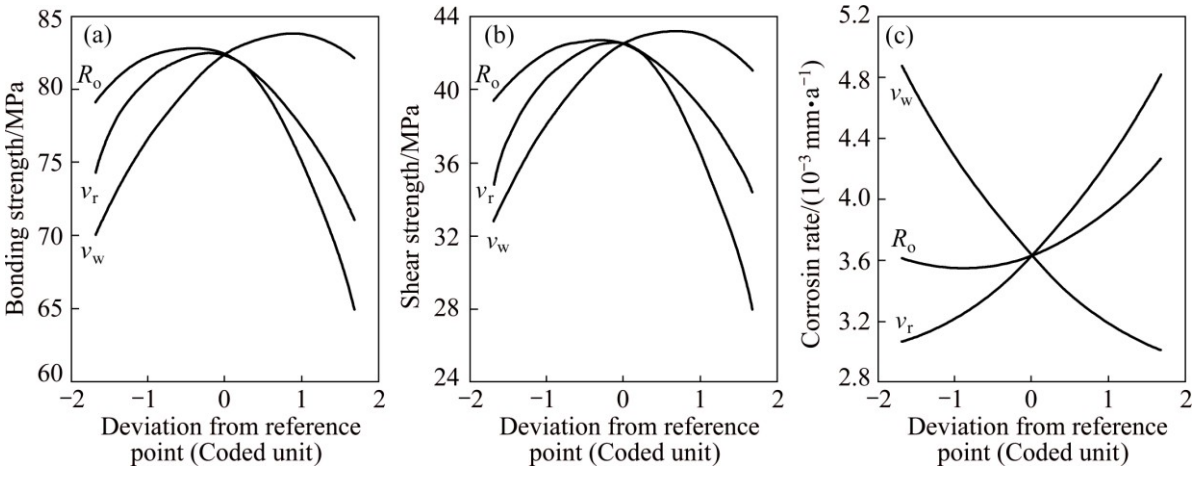

Fig. 3 Perturbation plots: (a) Bonding strength; (b) Shear strength; (c) Corrosion rate

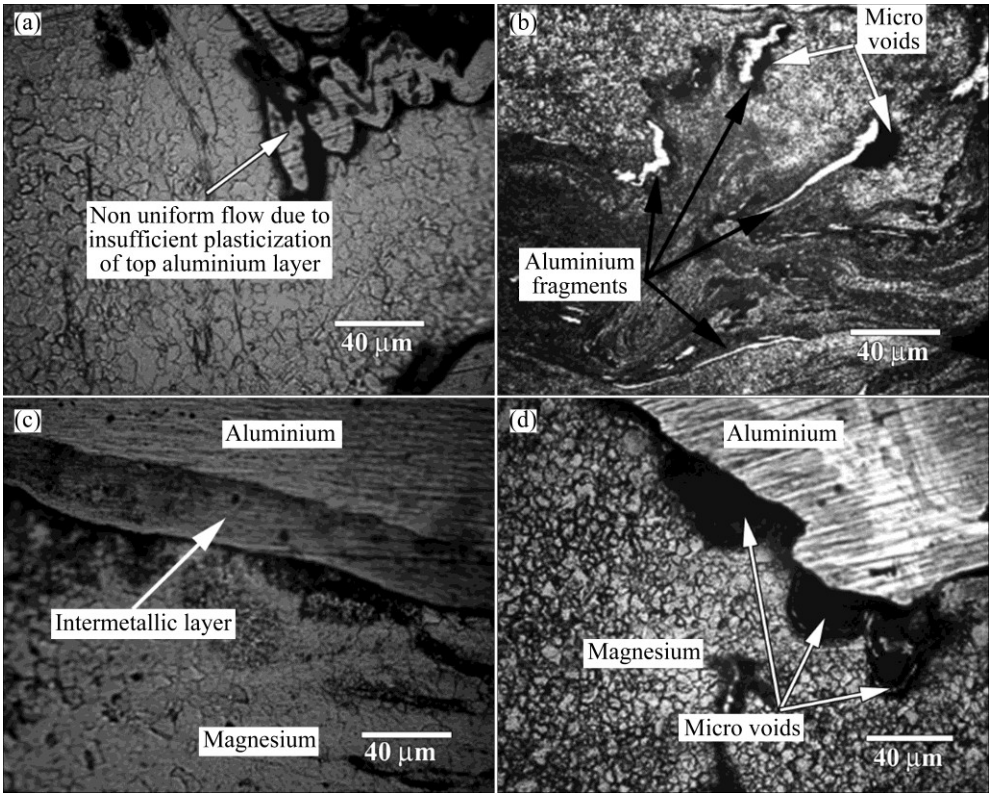

Fig. 4 Microstructures of Mg/Al dissimilar clads with inferior mechanical properties: (a) v_r<600 r/min; (b) v_r>1000 r/min; (c) v_w< 30 mm/min; (d) v_w>70 mm/min

At lower welding speed of 30 mm/min, heat generation was sufficiently high to cause grain coarsening and thicker intermetallic formation at the magnesium−aluminium interface (Fig. 4(c)), which resulted in very low bonding strength. On the other hand, a higher welding speed of 70 mm/min led to insufficient frictional heat and less exposure time for the diffusion to take place and subsequent metallurgical bonding at the interface (Fig. 4(d)). Though it was possible to obtain complete metallurgical bonding in the intermediate range of rotational and welding speeds without any micro cracks and voids, there was significant difference in joint strength at the interface and corrosion resistance of the top aluminium sheets. These variations in the properties strongly depend on intermetallic layer thickness, amount of intermixing between aluminium and magnesium in the pin influenced region and nature of mechanical interlocking at the interface. The intermetallic layer thickness increased with the increase of rotational speed and decrease in welding speed and subsequently lowered the joint interface strength due to higher heat input supplied. This is mainly due to the easier crack path along the intermetallic/matrix interface, which needed less energy for the propagation of cracks.

In multi-seam friction stir lap joining (i.e., cladding), overlap area is an essential process parameter, which greatly influences the joint strength. In this investigation for cladding of aluminium sheet on magnesium plate, shoulder diameter overlap ratio was considered instead of pin overlap ratio, which is very common in multi-pass friction stir processing technique for surface modification. The effective pin and shoulder overlap areas calculated at different pin overlap ratios are displayed in Fig. 5. It is interesting to note that, even for a least pin overlap ratio of zero, 69% of shoulder diameter area was overlapped. Since in this investigation, continuous multi-seam friction stir process without time

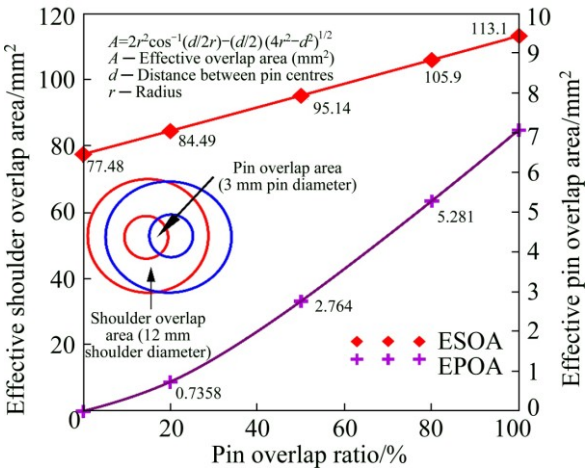

Fig. 5 Pin and shoulder overlap area comparison at different pin overlap ratios

gap between the subsequent passes was used, pin overlap ratio was avoided, which can lead to the formation of larger amount of intermetallic due to the exposure of larger overlap area under the shoulder diameter. The cross sectional macrostructures of multi-seam friction stir welded aluminium−magnesium clad joints are presented in Fig. 6.

For clads with 100% shoulder overlap ratio (i.e., two passes), the pin overlap area was also 100%. When the shoulder diameter overlap ratio was 80%, the pin overlap area was drastically reduced to 10%. For the other shoulder diameter overlap ratios considered, there was no pin overlap area existed. During friction stirring, the thin aluminium sheet was plasticized and flowed into the thick magnesium bottom sheet due to the taper pin profile, which formed pin influenced region. On the other hand, when tool pin was separated at a distance for two successive passes, interface between aluminium and magnesium was bonded due to the friction stir diffusion caused by shoulder influenced heat generation. A continuous and alternate arrangement of pin and shoulder influenced regions at clad interface formed a saw tooth profile similar to explosive welding. Also, a hook like feature was formed for the clad fabricated at 0, 20% and 100% of shoulder overlap ratio. However, for the clad joints fabricated at 100% of shoulder overlap ratio, saw teeth profile disappeared due to an additional pass to achieve complete overlap. It is observed that, the single pass clads at 0 and 100% of overlap ratio resulted in lower interface strength. Too low overlap yielded low interface strength due to improper metallurgical bonding between the aluminium top layer and magnesium bottom plate in the shoulder influenced regions. On the other hand, too close overlap increases the peak temperature of overlapping zone due to the preheating effect of previous pass, which can increase the possibility of liquation, rearrangement of intermetallic particles and grain coarsening. This results in weaker bonding at the aluminium−magnesium interfaces.

Though very good bonding was achieved for the clad joints fabricated at 80% overlap ratio, they showed lower bond and shear strengths due to the thinning of top aluminum layer (Fig. 6). Of the five overlap ratios used, the clad joints fabricated at 50% overlap ratio yielded superior bond and shear strength compared with its counterparts. To understand its characteristics, the microstructural features of different regions are further analyzed and presented in Fig. 7.

Sharp transition with significant mixing of Mg in Al was observed at the advancing side (Fig. 7(b)). On the

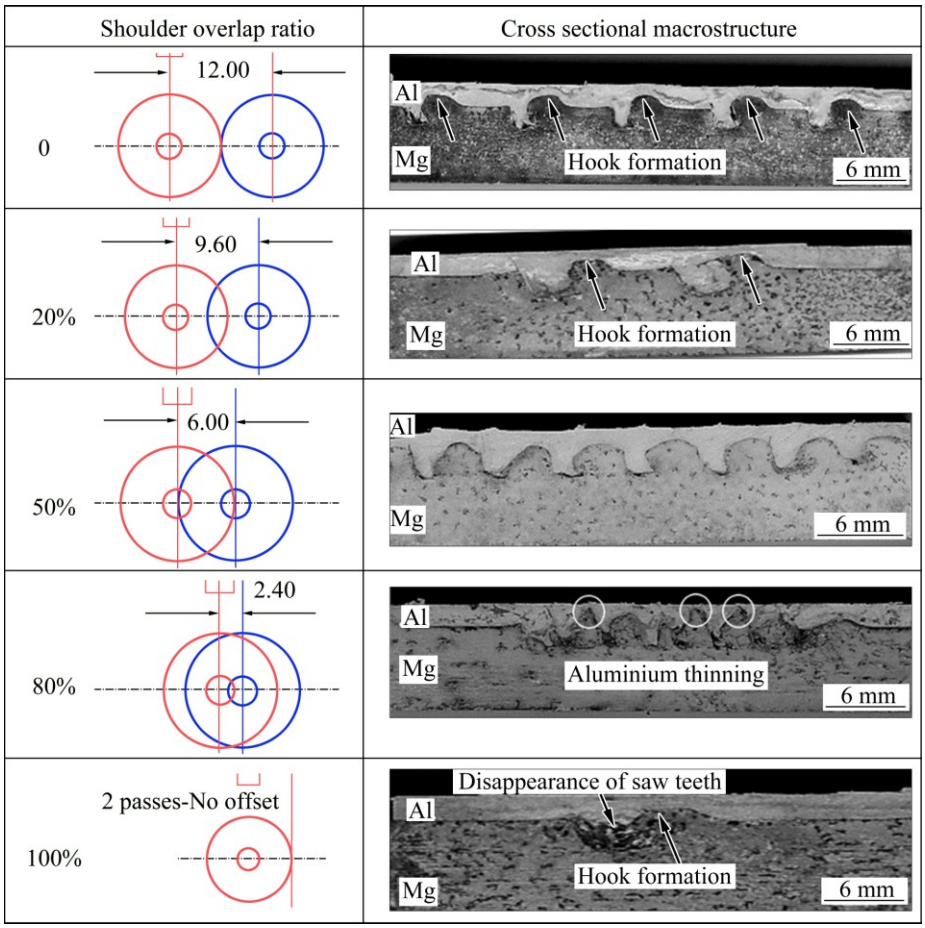

Fig. 6 Influence of shoulder overlap ratio at Mg/Al clad interface

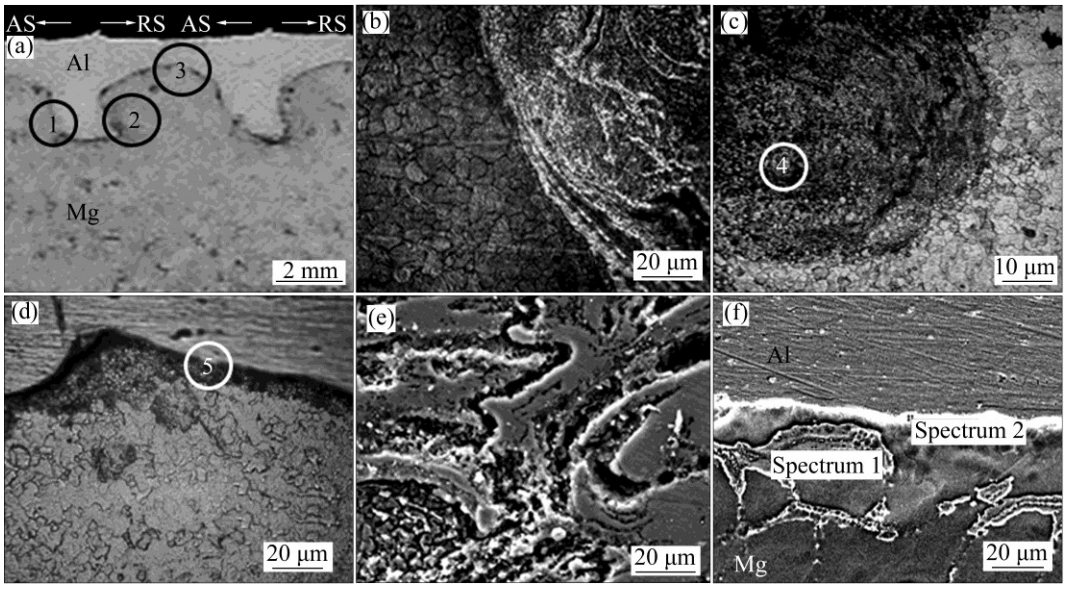

Fig. 7 Interface analysis by optical and scanning electron microscopy: (a) Macrostructure; (b) Region 1; (c) Region 2; (d) Region 3; (e) Region 4; (f) Region 5

other hand, at the retreating side, a curved interface with materials displaced towards the advancing side and swirl zone at the bottom is observed (Figs. 7(a) and (c)). Similarly at the shoulder influenced region, curved interface is observed due to the upward movement of magnesium towards the top aluminium sheet (Fig. 7(d)). This is mainly due to the exposure of previously stirred material to the second pass due to the tool shoulder overlap used.

Scanning electron microscopy was further used to understand the interface characteristics at the shoulder influenced region and swirl zone and the results are presented in Figs. 7(e) and (f). The swirl zone at the bottom of retreating side showed alternating layer of Al and Mg at the interface between them decorated with fine intermetallic particles (Fig. 7(e)). The Mg/Al interface at the shoulder influenced region (Fig. 7(f)) showed a thin continuous white layer and solidified irregular region in the magnesium side. SEM−EDS analysis indicated that, the thin continuous white layer consists of 63.14% Al and 36.86% Mg and irregular shaped region consists of 42.64% Al and 57.36% Mg. The compositions suggest that, the Al-rich thin continuous layer and Mg-rich irregular shaped regions are Al_3Mg_2 and $Al_{12}Mg_{17}$ intermetallic compounds, respectively. This indicated that, in addition to the mechanical locking, a strong metallurgical bond took place between the top aluminium sheet and lower magnesium plate. However, corrosion resistance of aluminium top is affected not by the intermetallic formation at the Mg−Al interface, instead, it is affected by amount of magnesium dilution in the aluminium top layer. The corrosion rate was high for clads which were fabricated at higher rotational speed, overlap ratio and lower welding speed. This is because of movement of heavily deformed magnesium layer and enhanced diffusion of magnesium from the lower plate to relatively thin aluminium top layer. Hence, the corrosion resistance of top aluminium layer depends on the amount of magnesium mixed due to the friction stirring.

5 Parameter optimization with multiple objectives

For the three responses considered, it is necessary to use the objective functions to achieve both maximization and minimization. Bond tensile strength and shear strength of clad joints need to be maximized. On the other hand, corrosion rate needs to be minimized, since it is an indication of environmental degradation. For numerical optimization, the goal for the process parameters such as rotational speed, welding speed and shoulder overlap ratio are kept in its range considered, whereas the goal for the responses is to maximize the σ_b, σ_c and to minimize the r_c. Design Expert V. 8.0 was used to optimize the process parameters, which uses downhill patter search algorithm to find an optimum solution around the stationary point to maximize or minimize the objective function. For multi response optimization, an overall desirability function needs to be calculated by combining the goals. In this study, numerical optimization was carried out using the desirability approach and the procedure can be dealt elsewhere [19]. A quick and methodical approach for multiresponse optimization for multi-seam friction stir cladding of dissimilar magnesium−aluminium alloy composite can

be done by superimposing or overlaying boundary limits of different responses as single contour plots. Superimposed contours were obtained by introducing the results obtained from the numerical optimization. This allows the users to visually select the optimum welding conditions according to the required criterion. The shaded area on the superimposed plot (Fig. 8) indicates the region which satisfies the proposed criteria and the optimized process parameters and the corresponding responses are displayed in Fig. 8.

Under the optimum processing conditions, the friction stir cladded dissimilar Mg/Al composite plates showed excellent ductility, which is also confirmed by bend test results presented in Fig. 9. It is clear that the cross sectional microstructure showed metallurgical mixing and crack-free interface.

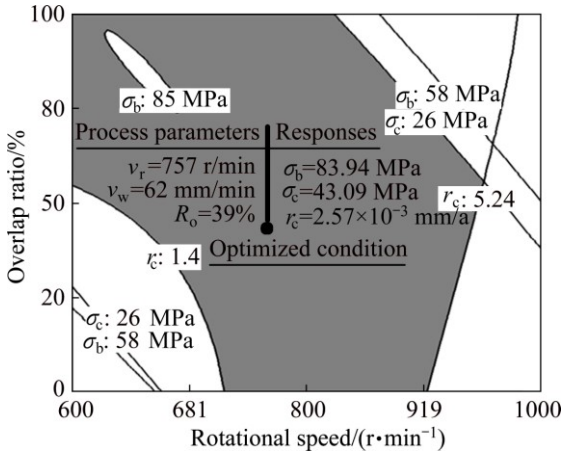

Fig. 8 Overlay plot of measured responses and their optimum values

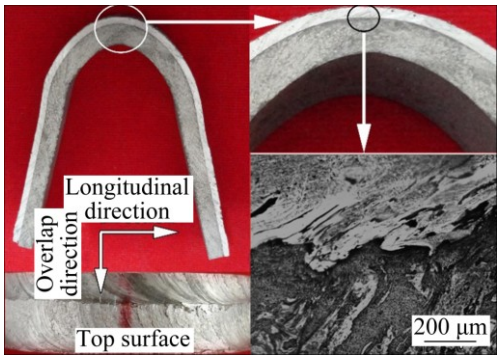

Fig. 9 Bend test results of Mg/Al dissimilar clads

6 Conclusions

1) Multi-seam friction stir cladded Mg/Al composite plate exhibits saw tooth-like interface similar to explosive welding. This is due to the alternate arrangement of pin influenced and shoulder influenced regions formed by multiple overlap passes.

2) At higher rotational and lower welding speeds, the clads exhibit inferior properties due to the defect caused by the entrapment of aluminium fragments, grain coarsening and formation of thicker intermetallic layer at the clad interface. Similarly, Mg/Al clads fabricated at too low rotational speed and too high welding speed result in weaker interface bonding due to the non-uniform aluminium flow and poor material mixing.

3) Shoulder overlap ratio has a significant effect on the nature of metallurgical bonding between the extruded magnesium bottom plate and top aluminium sheet in the advancing and retreating side and it is observed that, the retreating side consists of a swirl zone with alternating layers of aluminium and magnesium grains.

4) Multi-criterion optimization results show that, the Mg/Al clad composite plates fabricated at a rotational speed of 757 r/min, welding of 62 mm/min and shoulder overlap ratio of 39% yield a bond tensile strength of 84 MPa, shear strength of 43 MPa and corrosion rate of 2.57×10^{-3} mm/a. This is mainly due to improved metallurgical bonding and lower amount of magnesium diffused into the aluminium sheet top surface under optimized processing conditions.

References

[1] LUO A A. Magnesium casting technology for structural application [J]. Journal of Magnesium Alloys, 2013, 1: 2−22.

[2] GHALI E, DIETZEL W, KAINER K. General and localized corrosion of magnesium alloys—A critical review [J]. Journal of Material Engineering Performance, 2004, 13: 7−23.

[3] YAN T, TAN L, ZHANG B, YANG K. Fluoride conversion coating on biodegradable AZ31B magnesium alloy [J]. Journal of Material Science and Technology, 2014, 30: 666−674.

[4] HERNANDEZ-LOPEZ J M, NEMCOVA A, ZHONG X L, LIU H, ARENAS M A, HAIGH S J, BURKE M G, SKELDON P, THOMPSON G E. Formation of barrier-type anodic films on ZE41 magnesium alloy in a fluoride/glycerol electrolyte [J]. Electrochimica Acta, 2014, 138: 124−131.

[5] HU R, ZHANG S, BU J, LIN C, SONG G. Recent progress in corrosion protection of magnesium alloys by organic coatings [J]. Progress in Organic Coatings, 2012, 73: 129−141.

[6] PARDO A, CASAJUS P, MOHEDANO M, COY A E, VIEJO F, TORRES B, MATYKINA E. Corrosion protection of Mg/Al alloys by thermal sprayed aluminium coatings [J]. Applied Surface Science, 2009, 255: 6968−6977.

[7] VOLOVITCH P, MASSE J E, FABRE A, BARRALLIER L, SAIKAL W. Microstructure and corrosion resistance of magnesium alloy ZE41 with laser surface cladding by Al−Si powder [J]. Surface Coating Technology, 2008, 202: 4901−4914.

[8] JAFARIAN M, KHODABANDEH A, MANAFI S. Evaluation of diffusion welding of 6061 aluminum and AZ31 magnesium alloys without using an interlayer [J]. Materials and Design, 2015, 65: 160−164.

[9] ZHU B, LIANG W, LI X. Interfacial microstructure, bonding strength and fracture of magnesium–aluminum laminated composite plates fabricated by direct hot pressing [J]. Materials Science and Engineering A, 2011, 528: 6584−6588.

[10] CHANG H, ZHENG M Y, XU C, FAN G D, BROKMEIER H G, WU K. Microstructure and mechanical properties of the Mg/Al

multilayer fabricated by accumulative roll bonding (ARB) at ambient temperature [J]. Materials Science and Engineering A, 2012, 543: 249−256.

[11] LIU X B, CHEN R S, HAN E H. Preliminary investigations on the Mg−Al−Zn/Al laminated composite fabricated by equal channel angular extrusion [J]. Journal of Materials Processing and Technology, 2009, 209: 4675−4681.

[12] YAN Y B, ZHANG Z W, SHEN W, WANG J H, ZHANG L K, CHIN B A. Microstructure and properties of magnesium AZ31B–aluminium 7075 explosively welded composite plate [J]. Materials Science and Engineering A, 2010, 527: 2241−2245.

[13] BUFFA G, BAFFARI D, DI CARO A, FRATINI L. Friction stir welding of dissimilar aluminium–magnesium joints: Sheet mutual position effects [J]. Science and Technology of Welding and Joining, 2015, 20: 271−279.

[14] YAN Yong, ZHANG Da-tong, QIU Cheng, ZHANG Wen. Dissimilar friction stir welding between 5052 aluminum alloy and AZ31 magnesium alloy [J]. Transactions of Nonferrous Metals Society of China, 2010, 20: s619−s623

[15] LIU F, LIU Q, HUANG C, YANG K, YANG C, KE L. Microstructure and corrosion resistance of AZ80/Al composite plate fabricated by friction stir processing [J]. Material Science Forum, 2013, 747−748: 313−319.

[16] GANESA BALAMURUGAN K, MAHADEVAN K. Investigation on the effects of process parameters on the mechanical and corrosion behaviour of friction stir cladded AZ31B magnesium alloy [J]. Arabian Journal of Science and Engineering, 2015, 40: 1647−1655.

[17] MOHAMMADI J, BEHNAMIAN Y, MOSTAFAEI A, GERLICH AP. Tool geometry, rotation and travel speeds effects on the properties of dissimilar magnesium/aluminum friction stir welded lap joints [J]. Materials and Design, 2015, 75: 95−112.

[18] LAKSHMINARAYANAN A K, BALASUBRAMANIAN V. Comparison of RSM with ANN in predicting the tensile strength of friction stir welded AA7039 aluminium alloy joints [J]. Transactions of Nonferrous Metals Society of China, 2009, 1: 9−18.

[19] CANDIOTIA L V, de ZAN M M, CAMARA M S, GOICOECHE H C. Experimental design and multiple response optimization using the desirability function in analytical methods development [J]. Talanta, 2014, 24: 123−138.

异种镁铝合金多缝搅拌摩擦焊包覆接头的制备和性能评估

A. K. LAKSHMINARAYANAN; V. E. ANNAMALAI

Department of Mechanical Engineering, SSN College of Engineering,
Kalavakkam, Chennai 603110, Tamil Nadu, India

摘　要：建立了异种镁铝合金包覆接头连续多缝搅拌摩擦包覆工艺参数(旋转速度、焊接速度和重叠比)和质量表征(结合抗拉强度，剪切强度和腐蚀)的经验关系，研究了工艺参数对包覆性能的影响。采用多尺度优化过程得到了理想的加工条件，在该条件下制备得到的复合板具有较高的界面强度和较低的腐蚀速率。结果表明，薄的富铝连续层和不规则富镁区由金属间化合物 Al_3Mg_2 和 $Al_{12}Mg_{17}$ 组成，机械联锁的性质对接头界面强度有很大的影响。另一方面，在搅拌摩擦过程中镁混合到铝板的量对包覆接头的耐蚀性影响很大。弯曲测试表明，包覆接头具有优良的延展性。

关键词：搅拌摩擦包覆；异种接头；重叠比；优化

(Edited by Xiang-qun LI)